Journal of the European Ceramic Society 17 (1997) 623–640

PII: S0955-2219(96)00067-2
0955-2219/97/$17.00

Effect of Ageing Treatments at High Temperatures on the Microstructure and Mechanical Behaviour of 2D Nicalon/C/SiC Composites. 1: Ageing under Vacuum or Argon

C. Labrugère, A. Guette & R. Naslain

Laboratoire des Composites Thermostructuraux (UMR 47, CNRS-SEP-UB1), 3 allée de la Boëtie, Domaine Universitaire, 33600-Pessac, France

(Received 20 September 1995; revised version received 20 March 1996; accepted 28 March 1996)

Abstract

Two-dimensional Nicalon/C/SiC composites processed by chemical vapour infiltration have been aged at 1100–1500°C under vacuum or argon. The composites experience a weight loss $\Delta m/m_0$ related to the decomposition of the $SiO_{2x}C_{1-x}$ phase of the fibres and to side-reactions between the fibre decomposition gaseous products (particularly SiO) and carbon (from the fibre and the interphase), as assessed by electron probe microanalysis, and Auger electron spectroscopy analyses. This decomposition/reaction process results in an evolution of the mechanical behaviour (characterized through tensile/push-out tests) correlated with the weight loss. Mild ageing conditions ($\Delta m/m_0 < 1{\cdot}3\%$) result in a weakening of the fibre–matrix bonding due to some interfacial decohesion with a decrease in both the proportional limit and failure strength, as well as an increase in the failure strain. More severe ageing conditions ($\Delta m/m_0 \approx 2\%$) yield a partial consumption of the interphase with the formation of large SiC-crystals on the fibre surface weakening the fibres, the composite still exhibiting a non-linear mechanical behaviour. Finally, for extremely severe ageing conditions ($3 < \Delta m/m_0 < 7\%$), the interphase is totally consumed and the fibres undergo a pronounced decomposition/crystallization process, the composite becoming brittle with a very low load-bearing capability. © *1997 Elsevier Science Limited. All rights reserved.*

Résumé

Des composites 2D-Nicalon/C/SiC élaborés par CVI ont été vieillis entre 1100 et 1500°C sous vide ou sous argon. Les composites présentent une perte de masse $\Delta m/m_0$ relative à la décomposition de la phase $SiO_{2x}C_{1-x}$ des fibres, et à des réactions complémentaires entre les produits gazeux de la décomposition de la fibre (en particulier SiO) et le carbone (de la fibre et de l'interphase), comme le montrent les analyses EPMA, TEM/EELS et AES. Ce processus de décomposition/réaction entraîne une évolution du comportement mécanique (caractérisé par des essais de traction et d'indentation-push-out), fonction de la perte de masse. Des conditions de vieillissement peu sévères ($\Delta m/m_0 < 1{\cdot}3\%$) conduisent à un affaiblissement de la liaison fibre/matrice, dû à des décohésions interfaciales, accompagné par une diminution simultanée de la limite élastique et de la contrainte à rupture, ainsi que par une augmentation de l'allongement à rupture. Des conditions de vieillissement plus sévères ($\Delta m/m_0 \approx 2\%$) entraînent une consommation partielle de l'interphase avec formation de cristaux de SiC de grande dimension sur la surface de la fibre affaiblissant les fibres, et conférant au composite un comportement mécanique non-élastique. Enfin, pour des conditions de vieillissement draconiennes ($3 < \Delta m/m_0 < 7\%$), l'interphase est totalement consommée, et les fibres présentent un processus de décomposition/cristallisation prononcé, le composite devenant fragile avec une très faible tenue à la rupture

1 Introduction

SiC/SiC composites consist of SiC-based continuous ceramic fibres embedded in a SiC matrix. They exhibit non-brittle mechanical behaviour when the fibres are bonded to the matrix via a thin layer of a compliant material, e.g. a thin film

of pyrocarbon, referred to as the *interphase*. SiC/SiC composites have been designed to withstand long exposures at high temperatures in oxidizing atmospheres on the basis of the high melting point of SiC ($T_d \approx 2500°C$) and the formation of a silica protective layer (passive oxidation regime). They are expected to replace carbon–carbon composites, known to exhibit very poor oxidation resistance, in the aerospace industry (e.g. as rocket or jet engine parts or as thermal protection of structures).

In SiC/SiC composites, the fibres that are presently used, are usually not pure SiC fibres. The most commonly used, i.e. Si–C–O fibres, are made from a polycarbosilane (PCS) precursor according to a spinning/oxygen curing/pyrolysis process developed by Yajima *et al.*[1] The oxygen, which is introduced in the fibre during the curing step (in order to make the green PCS fibre infusible), is not eliminated during the following pyrolysis step performed at about 1200°C, owing to the stability of the Si–O bond. As a result, ex-PCS fibres prepared according to the Yajima route, such as Nicalon fibres*, belong to the ternary Si–C–O system (their overall composition being close to 53·6% Si, 31·5% C, 14·9% O, by weight). In the as-prepared state, Nicalon fibres consist of SiC nanocrystals (mean size: 2 nm) in a matrix of amorphous silicon oxycarbide. They also contain a small amount of free carbon as basic structural units (BSU)† as well as trace amounts of hydrogen thought to be bonded to carbon.[2-5] It is now well established that Si–C–O (ex-PCS) fibres are metastable at high temperatures. They undergo decomposition with an evolution of gaseous species (mainly CO and SiO) when heated beyond about 1100°C.[6,7] Their evolution towards the stable thermodynamic state is progressive with a rate that depends on temperature, pressure and the nature of the atmosphere.[8-18]

SiC/SiC composites also contain a pyrocarbon interphase which is not inert chemically since it can react with the decomposition products of the fibres (i.e. CO and SiO) and with the atmosphere when the materials are exposed to oxidizing atmospheres at high temperatures. As a result, dramatic changes may occur in the fibres and the fibre–matrix (FM) interfacial zones when SiC/SiC composites are aged under such conditions, which may in turn alter significantly their non-brittle mechanical behaviour.

The aim of the present work was first to study the change occurring in the Nicalon fibres and the pyrocarbon (PyC) interphase when SiC/SiC composites were aged at temperatures (i.e. 1100–1500°C) higher than the processing temperature (≈ 1000°C) and under various atmospheres. In a second step, it was also to derive a correlation between the evolution of the FM interfacial zone and the change in the mechanical behaviour. The results are presented in two related articles, the first dealing with ageing performed under vacuum or inert atmosphere (argon) and the second with ageing treatments in reactive atmosphere (i.e. containing CO). The effect of a SiC seal-coating, the main effect of which is to entrap the decomposition products of the fibres, is also studied in the second part.

*Nicalon fibres (ceramic grade) from Nippon Carbon, Japan.
†A BSU is a stack of a few carbon layers of limited lateral size.

2 Experimental

2.1 Materials

The starting materials used in the present study are composites fabricated (by SEP, Le Haillan, France) from Nicalon fabrics (NLM 202 Nicalon fibres, from Nippon Carbon, Japan). Thus the composites exhibit a bidirectional fibre architecture, and will be referred to as two-dimensional (2D) SiC/C/SiC, with a fibre volume fraction of about 40%. The materials were fabricated according to a three-step process. In a first step, a 2D fibre preform was prepared from a stack of fabrics maintained pressed together with a graphite tooling, in order to fix the fibre volume fraction. Then, the interphase material (i.e. a film of about 0·1 μm of pyrocarbon) was deposited *in situ* on the fibre surface, from the cracking of a hydrocarbon precursor (mainly CH_4). Finally, the SiC matrix was formed *in situ* by chemical reaction from a mixture of CH_3SiCl_3 and hydrogen, the residual porosity being 10–15%. The infiltration of both the PyC interphase and the SiC matrix was performed according to the isothermal/isobare chemical vapour infiltration technique (ICVI), which has been described in detail elsewhere.[19] It is sufficient to recall here that in ICVI both the temperature and the pressure have to be low enough (i.e. values as low as ≈ 1000°C and a few kPa, respectively) to avoid early plugging of the pore entrances by the deposit and to achieve in-depth homogeneous infiltration.[19]

Rectangular samples (100 × 10 × 3 mm^3) were cut with a diamond saw from the composite plates and were shaped, as shown in Fig. 1, for the ageing treatments and the mechanical tensile tests. The length of the sample was orientated along one of the fibre directions of the fabric (direction 1 or 2). The samples were used in the as-cut state, i.e. no protective surface coating was applied to the sample surface before the ageing treatments, in this first part of the study.

2.2 Ageing treatments

The ageing treatments were performed directly on the tensile test specimens with the apparatus shown schematically in Fig. 2. The specimen was treated in a graphite crucible heated by induction of radio frequency (RF) current (the crucible acting as susceptor), in order to reach high temperatures in a short time (i.e. 1100–1500°C within less than 15 min). For the treatments under vacuum, the ageing chamber was evacuated with a turbomolecular pump residual pressure: 10^{-1} to 10^{-3} Pa) whereas those in argon were performed at constant volume under a pressure slightly lower than atmospheric pressure. The ageing conditions are listed in Table 1.

The relative weight variations, $\Delta m/m_0$ (where $m_0 \approx 8$ g is the initial weight of a tensile test specimen), occurring during the ageing treatment were continuously recorded with a microbalance (D101 from Cahn, USA; sensitivity: 0·1 μg).

2.3 Characterization

Analysis of the FM interfacial zone (in terms of chemical composition and microstructure) was performed by transmission electron microscopy (TEM) (2000 FX from Jeol, Japan) coupled to electron-energy loss spectroscopy (EELS) (300 kV TEM from Philips and PEELS from Gatan) and by Auger electron spectroscopy (AES) (PHI-590 from Perkin–Elmer). The samples used for TEM characterization were cut with a diamond wire saw, from aged specimens that had been subjected to tensile testing, at a distance of about 15 mm from the failure surface as shown schematically in Fig. 1. The specimens were thinned according to the classical procedure for this kind of material (i.e. mechanically, down to 80–150 μm, and then with Ar^+ ions). AES analyses were performed in the depth profiling mode (Ar^+ ion etching) on the surface of pulled-out fibres present at the failure surface of tensile test specimens. The Auger electron transitions used are: Si_{LVV} (referred to as Si1) for silicon; C_{KLL} (referred to as C1) for carbon and O_{KLL} (referred to as O1) for oxygen. The apparent atomic concentrations were calculated from the peak-to-peak heights of the spectra recorded in the derivative $dN(E)/dE$ mode. The sensitivity

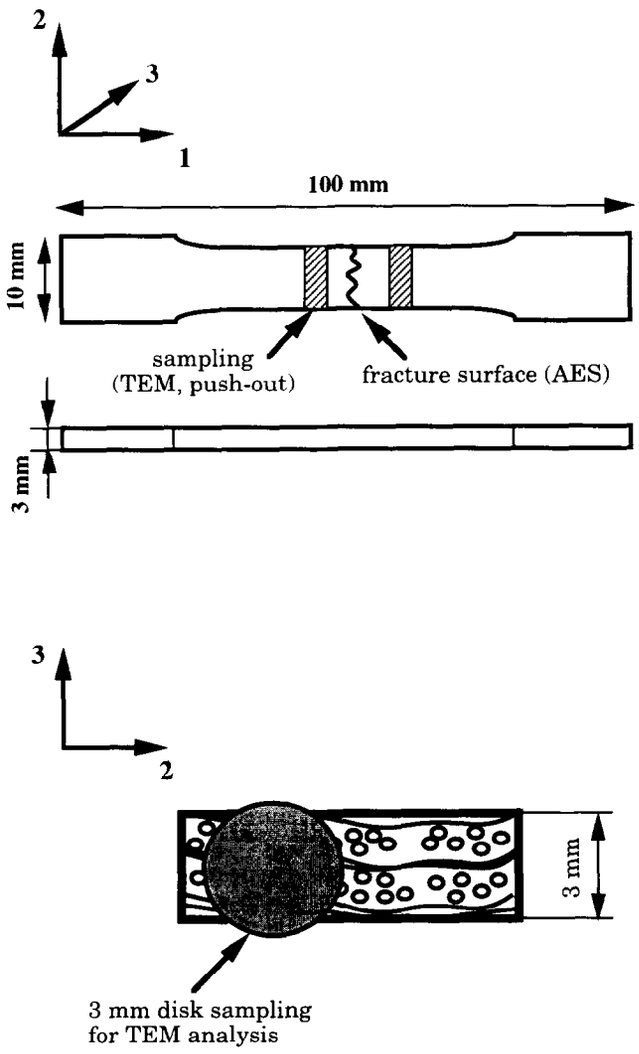

Fig. 1. Location of the specimens used for the TEM, AES and push-out characterization, in a failed tensile test specimen.

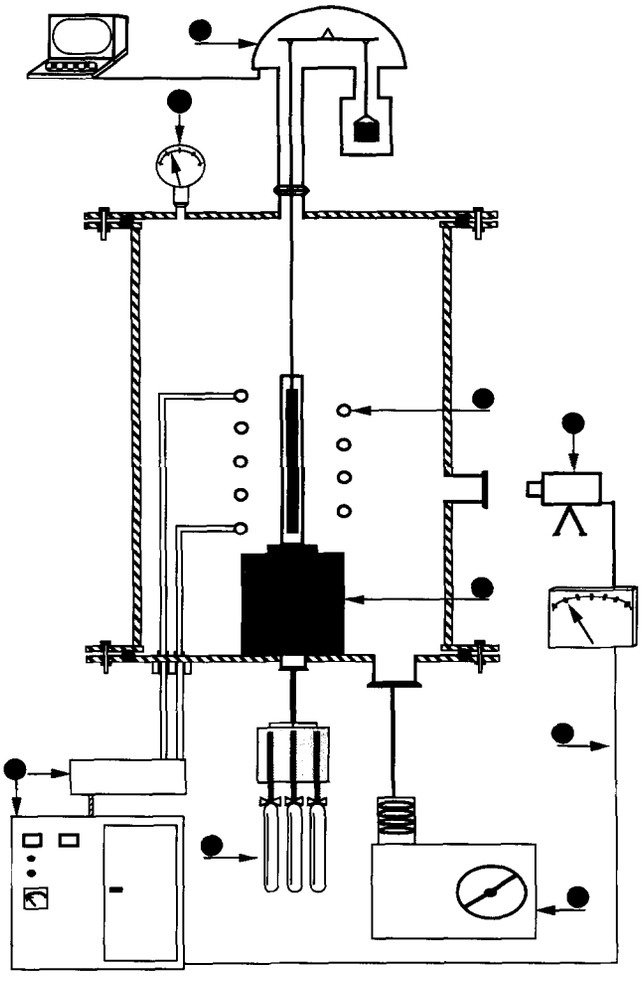

Fig. 2. Apparatus used for the ageing treatments (schematic): 1–RF power supply; 2—induction coil; 3–optical bicolour pyrometer; 3'—temperature regulation; 4—microbalance; 5—insulating holder; 6—turbomolecular pump; 6'—pressure gauge; 7—gas lines.

Table 1. Conditions used for ageing treatments of the tensile specimens and corresponding weight loss

Materials reference	*Ageing atmosphere (Pa)*	*Ageing temperature (°C)*	*Ageing time (h)*	$\Delta m/m_0$ *(%)*
0 (as-received)	none	none	none	none
1 (aged)	vacuum (6×10^{-2})	1100	50	−0·55
2 (aged)	vacuum (6×10^{-2})	1100	90	−1·3
3 (aged)	vacuum (1×10^{-1})	1200	20	−2·05
4 (aged)	vacuum (1×10^{-3})	1200	94	−6·3
5 (aged)	vacuum (2×10^{-2})	1300	1	−1·5
6 (aged)	vacuum (5×10^{-3})	1300	1·5	−3·0
7 (aged)	vacuum (2×10^{-3})	1300	24	−6·9
8 (aged)	vacuum (2×10^{-2})	1460	0·08	−0·27
9 (aged)	vacuum (2×10^{-2})	1460	3	−9·3
10 (aged)	argon (7×10^{4})	1100	29	−0·37
11 (aged)	argon (7×10^{4})	1200	49	−3·58
12 (aged)	argon (7×10^{4})	1300	24	−6·39

factors were adjusted with respect to the results obtained by electron probe microanalysis (EPMA).

The elemental composition of the fibre, near the FM interfacial zone, was assessed by EPMA characterization (CAMEBAX instrument from Cameca, France) performed on one polished face of aged specimens. Both carbon and oxygen were analysed with a wavelength dispersion spectrometer (WDS) (C K_α and O K_α peaks), an ODPB monochromator and standards of carbon and silica. Silicon was analysed with an energy dispersion spectrometer (Si K_α peak) and a standard of SiC. The results will be shown as radial concentration profiles.

The tensile tests were performed on aged specimens, at ambient temperature and with a constant strain rate of 0·05% min^{-1}, using an Instron 8501 tensile tester. The FM bond strength was assessed by push-out tests performed on material slices (with a thickness of 300 μm or less) cut from failed tensile test specimens according to a procedure identical to that described for the TEM specimens. The indentation device (indentor licensed from ONERA, France) consisted of a Vickers diamond tip equipped with a capacitive displacement sensor. The load applied to the diamond tip was measured with an inductive load cell (maximum capacity: 2 N) set below the sample. The tests were run with indentation rates of the order of 0·12 $\mu m\ s^{-1}$.

3 Results

3.1 As-fabricated 2D SiC/C/SiC composites

2D SiC/C/SiC, fabricated from Nicalon fibres according to the ICVI process, is a family of composites that have been the subject of many studies. Their mechanical properties depend closely on the processing conditions.[20,21] Thus, the as-received composites were first characterized (from chemical and mechanical points of view) in order to assess the class to which they belong within the 2D SiC/C/SiC family.

Within the as-received composites, the Nicalon fibres exhibit a mean diameter of 14 μm and a chemical composition (established from EPMA data) close to 35 at% Si, 48 at% C and 17 at% O (hydrogen thought also to be present was not analysed). Each fibre is surrounded by a thin amorphous layer (thickness in the range 5–10 nm), as shown in Fig. 3, which has been assigned to a mixture of silica and carbon on the basis of AES concentration profiles recorded from the surface of pulled-out fibres present at the failure surface of tensile test specimens (Fig. 4). Additionally, the energy corresponding to the Si_{LVV} Auger electron

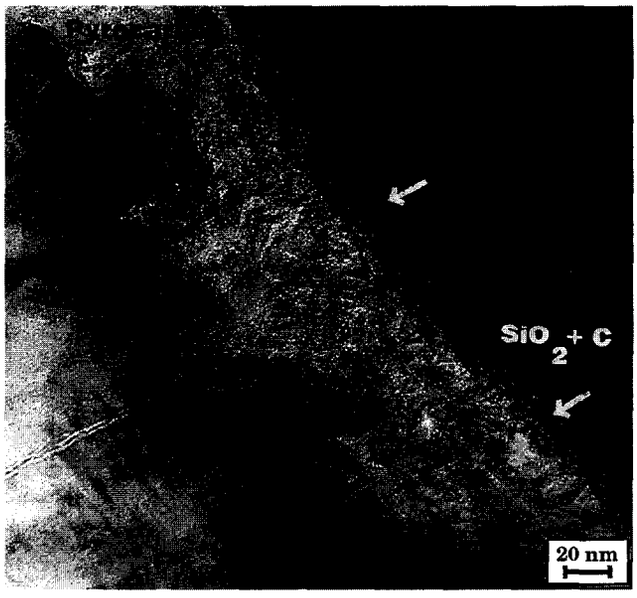

Fig. 3. TEM image (bright-field) of the FM interfacial zone in the as-received 2D SiC/C/SiC composite.

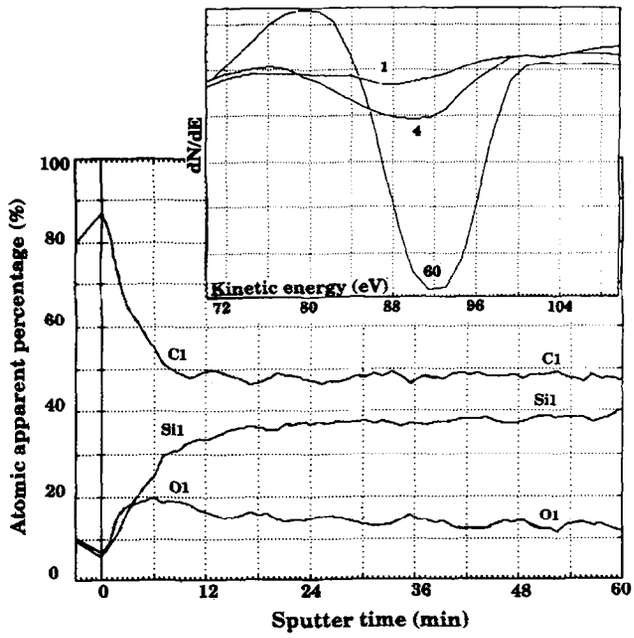

Fig. 4. AES concentration depth profiles recorded radially from the surface of a pulled-out fibre present at the failure surface of an as-received 2D SiC/C/SiC composite, with an etching rate of 5 nm min^{-1} (standard: Ta_2O_5). Inset: shift of the Si_{LVV} transition as a function of etching time (i.e. after 1, 4 and 60 min of etching).

transition is observed to change when moving from the surface of the fibre to the core, i.e. from 88 to 92 eV (inset in Fig. 4). This feature is consistent with the occurrence of silicon atoms bonded to oxygen near the fibre surface. This amorphous layer might be the result of some decomposition of the fibre during processing (of the fibre itself or/and of the composite), as suggested by previous authors.[21]

The pyrocarbon interphase deposited by ICVI exhibits a thickness of about 0·1 μm and consists essentially of a quasi-isotropic nanoporous carbon (Fig. 3). However, near the fibre surface (i.e. over a thickness of about 20 nm), the carbon atomic layers tend locally to be orientated parallel to the fibre surface, as previously reported by Cojean *et al.* for similar composites.[20]

The as-received 2D SiC/C/SiC composite exhibits in tensile loading a mechanical behaviour with a limited non-linear domain. The Young's modulus corresponding to the elastic domain is close to 230 GPa. The material fails at somewhat low failure strain (i.e. 0·17%) and low failure stress (i.e. 150 MPa).

From all these data, it can be concluded that the 2D SiC/C/SiC composites used as starting material in the present study belong to a class of composites referred to type C[20] or type III,[21] characterized by a moderate FM bond strength and in which an early failure of the fibres (possibly damaged during processing) results in a low composite failure strain (typically 0·16–0·25%).[20]

3.2 Weight loss during the ageing treatments

The variations of the weight loss, $\Delta m/m_0$ experienced by the tensile specimens during the ageing treatments are shown as a function of time in Fig. 5. The weight loss depends strongly on temperature and to a less extent on the atmosphere (vacuum or argon). For the ageing durations considered here, the weight loss becomes significant beyond 1200°C. At 1300°C and under vacuum, the weight loss $\Delta m/m_0$ rapidly becomes higher than 5%. Furthermore, a maximum weight loss close to 11% has been observed for 1550°C. This maximum weight loss, when expressed with respect to the weight of the fibres alone, i.e. as $\Delta m/m_f$ (where m_f is the weight of the fibres in the composite calculated for V_f = 40%), yields a value of about 27%. Under a pressure of argon (70 kPa), the variations of $\Delta m/m_0$ as a function of time exhibit the same features, the weight loss rate being lower than that observed under vacuum as long as the temperature remains lower than 1300°C.

For the purpose of comparison, similar ageing treatments were performed directly on the Nicalon fabrics (i.e. without PyC interphase and SiC matrix). The results (Fig. 6) clearly show that, for given ageing conditions, the weight loss rate is much higher for the unembedded fibres, thus

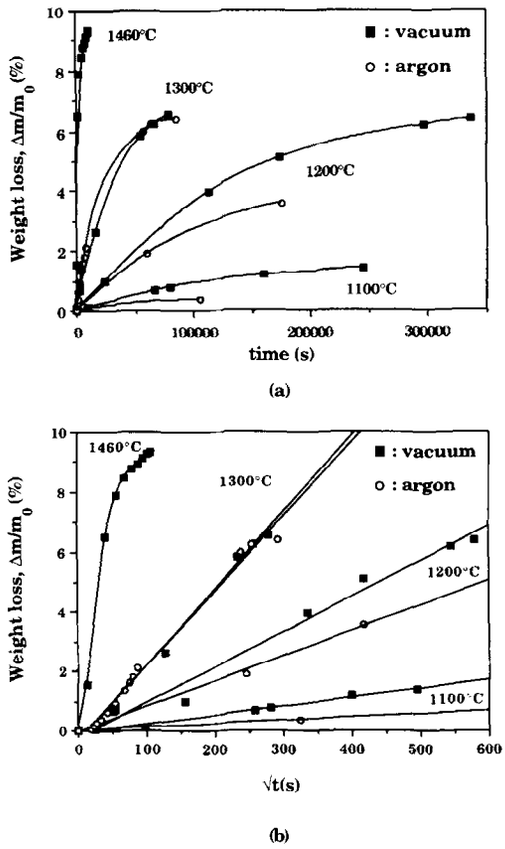

Fig. 5. Weight loss experienced by 2D SiC/C/SiC tensile specimens during ageing treatments performed under vacuum (residual pressure: 10^{-1} to 10^{-3} Pa) or under a pressure of argon (70 kPa): (a) as a function of time and (b) as a function of the square root of time.

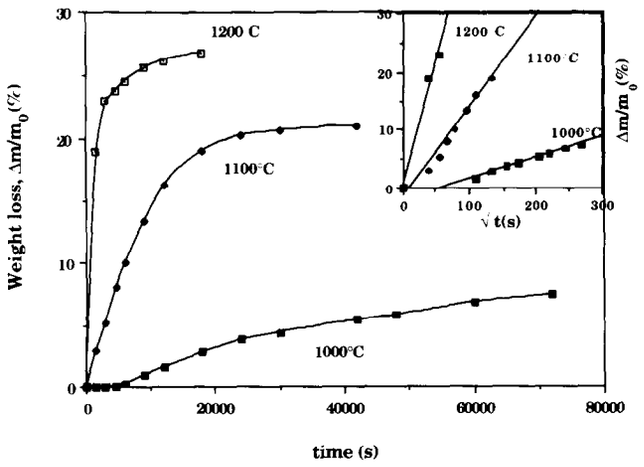

Fig. 6. Variations of the weight loss, $\Delta m/m_0$, experienced by Nicalon fabric specimens ($m_0 \approx 0{\cdot}25$ g) as a function of time during ageing treatments performed under vacuum (residual pressure: 10^{-3} Pa). In the inset: variations of $\Delta m/m_0$ as a function of $t^{1/2}$.

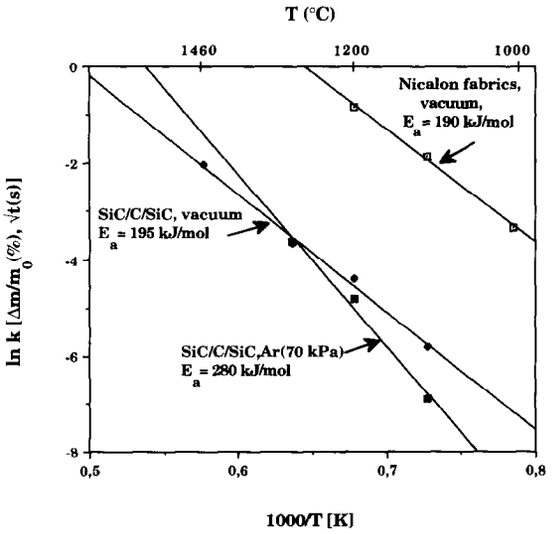

Fig. 7. Variations of the diffusion-based constant k as a function of reciprocal temperature (Arrhenius plot) related to ageing treatments performed on Nicalon fabrics or 2D SiC/C/SiC composites, under vacuum or argon.

suggesting that the PyC + SiC coating entraps the fibre decomposition products and slows down the decomposition process. Furthermore, at the lowest ageing temperature, i.e. 1000°C, an induction period (during which no weight loss occurs) of about 100 min is observed.

The variations of the weight loss, $\Delta m/m_0$, as a function of the square root of time are shown in Fig. 5(b) for the tensile composite specimens and in the inset of Fig. 6 for the Nicalon fabrics. These variations are linear, at least to a first approximation, both under vacuum and argon for $T \leq 1300$°C (with the restriction related to the induction period for the Nicalon fabrics, mentioned above). However, this linear variation is no longer obeyed at higher temperatures (e.g. 1460°C) under vacuum [Fig. 5(b)]. These data suggest that the phenomenon responsible for the weight loss (in the unembedded fibres and in the composites) may be rate-controlled by a diffusion step. Diffusion-based constants k can be defined as the slopes of the straight lines shown in Figs 5(b) and 6. Their thermal variations, expressed as Arrhenius plots, are shown in Fig. 7. The apparent activation energies are similar for the fibres and the composites aged under vacuum (i.e. $E_a \approx 190$ kJ mol^{-1}) whereas that for the composites aged under a pressure of argon ($E_a \approx 280$ kJ mol^{-1}) is significantly higher.

3.3 Chemical and microstructural analysis of the fibre and FM interfacial zone in aged composites

The ageing treatments have an effect on: (i) the SiC grain size in the fibre, (ii) the chemical composition of the fibre and (iii) the nature of the FM interfacial zone, which is directly related to the importance of the weight loss experienced by the composite. This is almost similar for the composites aged under vacuum and for those treated under a pressure of argon, for a given $\Delta m/m_0$ value [which means different ageing times, for $1100 < T < 1200$°C, as shown in Fig. 5(a)]. Thus, these various effects will be described in the following only for the composites which have been aged under vacuum.

3.3.1 SiC grain size in the fibres

As shown in Figs 8 and 9, the size of the SiC crystals in the fibre (as derived from the TEM images) increases as the weight loss experienced by the composite increases. In the as-received composites, it ranges from 1 to 2·5 nm, a value which is close to those reported previously for the Nicalon fibre (ceramic grade) itself.[2–4,17,18,22] As long as the weight loss remains low enough, e.g. for $\Delta m/m_0 = 0{\cdot}5\%$ (corresponding to an ageing treatment of 50 h at

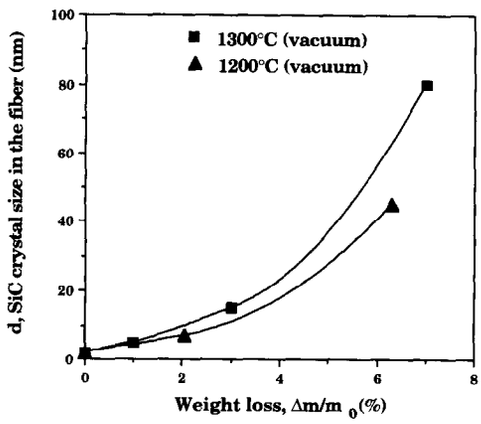

Fig. 8. Correlation between SiC crystal size (as derived from TEM images) and weight loss experienced by 2D SiC/C/SiC composites during ageing treatments performed under vacuum (residual pressure: 10^{-1} to 10^{-3} Pa).

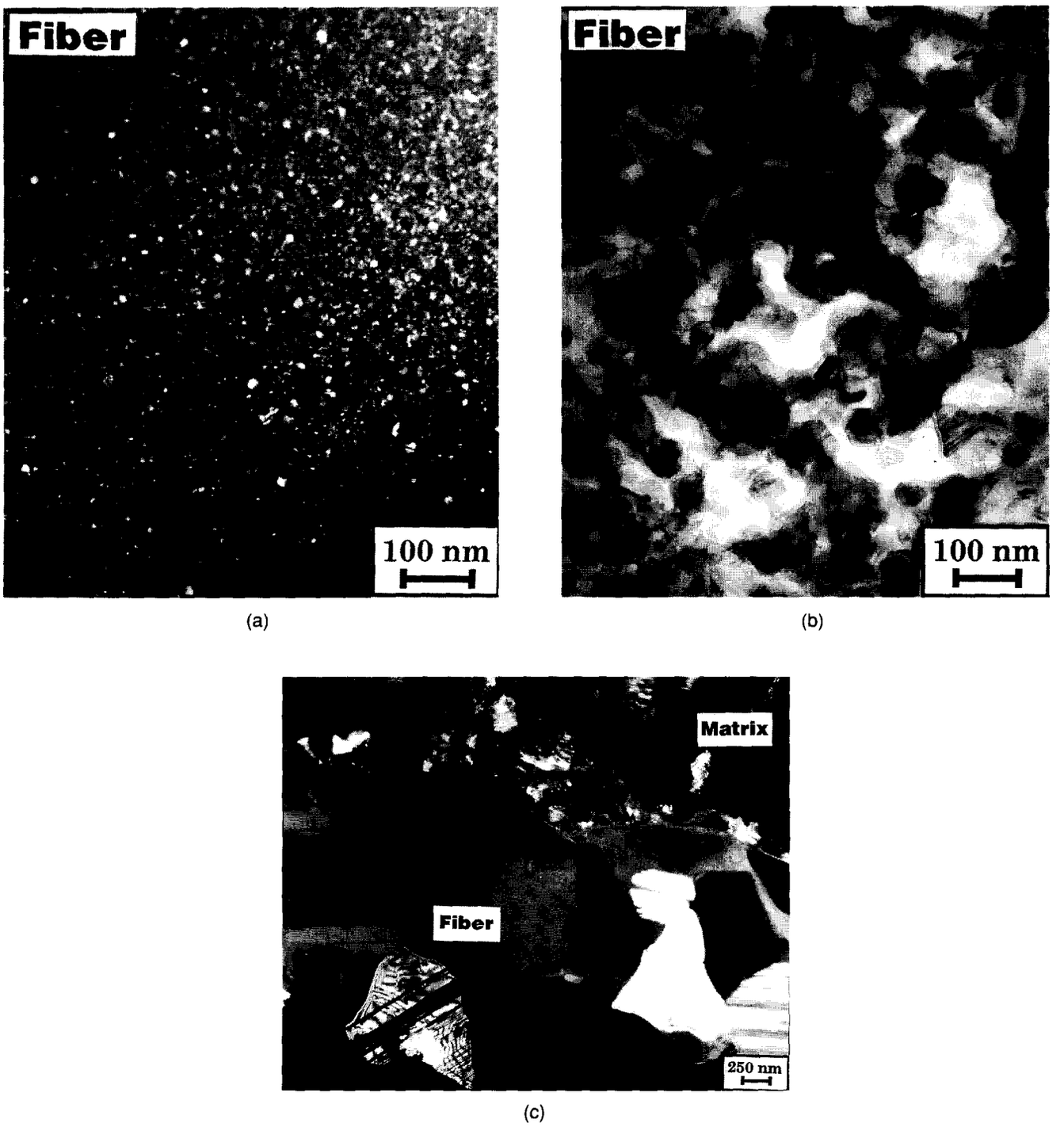

Fig. 9. TEM images showing SiC grain growth in Nicalon fibres for 2D SiC/C/SiC composites aged under vacuum (residual pressure: 10^{-1} to 10^{-3} Pa) with increasing weight loss: (a) $\Delta m/m_0 = -2\%$ (1200°C, 20 h) (dark-field SiC_{111}); (b) $\Delta m/m_0 = -6{\cdot}3\%$ (1200°C, 94 h) (bright-field); and (c) $\Delta m/m_0 = -9{\cdot}3\%$ (1460°C, 3 h) (dark-field SiC_{111}).

1100°C), the SiC grain size in the fibres is almost unchanged. Conversely, for more severe ageing treatments (i.e. beyond 1200°C), the SiC crystals undergo significant growth which is associated with chemical degradation of the fibres.[8,13,17] As an example, the crystal size is 40–80 nm when $\Delta m/m_0$ is equal to 6–7% (for ageing treatments at 1200–1300°C) [Figs 8 and 9(b)] and reaches a value as high as 1 μm for a sufficiently long treatment at 1460°C [Fig. 9(c)]. Finally, it is worth noting that the SiC grain size is almost the same, for a given $\Delta m/m_0$ value, in materials aged at 1200 and 1300°C.

3.3.2 FM interfacial zone and fibre surface

For mild ageing treatments (e.g. 50–90 h at 1100°C; $\Delta m/m_0 = 0{\cdot}5$–1%), the pyrocarbon interphase does not undergo significant microstructural change. It still consists of quasi-isotropic nanoporous carbon in the bulk with a thin layer (20–30 nm) of anisotropic carbon on the fibre side [Fig. 10(a)]. Additionally, decohesions [arrows in

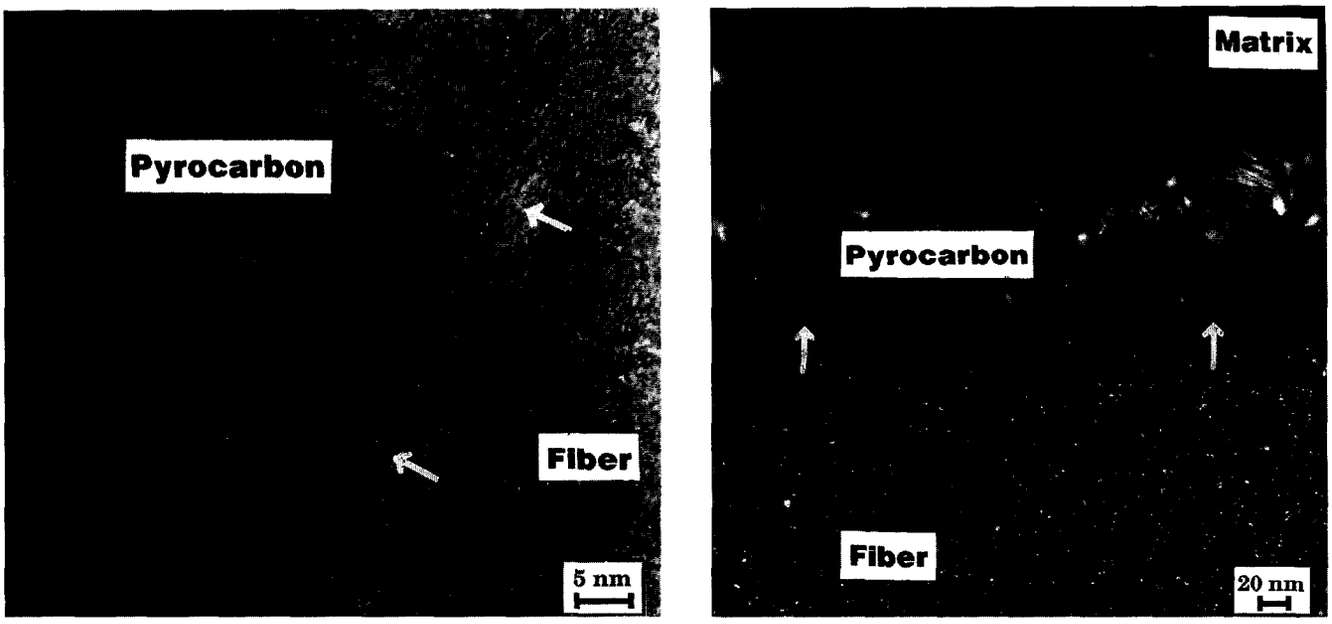

Fig. 10. TEM images of the FM interfacial zone in 2D SiC/C/SiC composites aged for 50 h at 1100°C under vacuum (residual pressure: 6×10^{-2} Pa): (a) lattice fringe image and (b) dark-field (SiC_{111}) image. Arrows show decohesions between the anisotropic carbon layer and the fibre surface.

Figs 10(a), (b)] are present locally between the fibre surface and the anisotropic carbon layer. As already observed for the as-received composites (Section 3.1), the fibre surface consists (over a thickness of about 10 nm) of an amorphous mixture of silica and carbon (as supported by AES and PEELS data). The AES depth concentration profiles (Fig. 11) show an increase in both the oxygen and carbon concentrations near the fibre surface. Additionally, there is a shift (from ≈90 to ≈93 eV) of the Si_{LVV} transition when moving in-depth, suggesting that silicon is mainly bonded to oxygen (as in silica) very near the fibre surface (inset in Fig. 11). In a complementary manner, the PEELS data (Table 2) also show an increase in the O/Si atomic ratio in the amorphous skin surrounding the fibre (the oxygen level within this area being slightly higher than for the as-received composites). Finally, when moving inward (Fig. 11), the chemical composition rapidly becomes similar to that in the as-supplied composites (with, however, a slightly lower oxygen concentration). In a similar manner, the size of the free carbon BSUs in the fibre (i.e. four or five distorted carbon layers (≈ 1 nm in width) stacked together) is close to

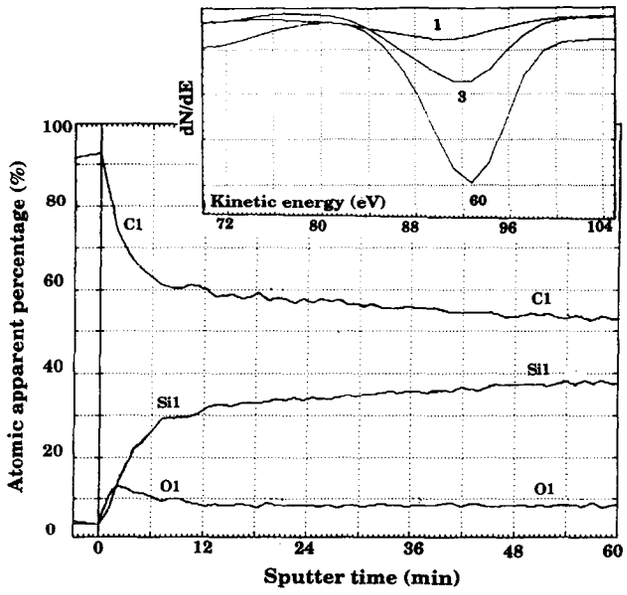

Fig. 11. AES depth concentration profiles recorded from the surface of a pulled-out fibre present at the failure surface of a tensile specimen of a 2D SiC/C/SiC composite aged for 90 h at 1100°C under vacuum (residual pressure: 6×10^{-2} Pa). The etching rate was 8 nm min^{-1} (reference: Ta_2O_5). The shift of the Si_{LVV} transition as a function of etching time (1, 3 and 60 min) is shown in the inset.

Table 2. O/Si and C/Si atomic rations as assessed by PEELS analysis near the surface Nicalon fibres in thin foils of 2D SiC/C/SiC composites aged under various conditions

Ageing treatment	*Distance from fibre surface (nm)*	*O/Si at. ratio*	*C/Si at. ratio*
1100°C 90 h vacuum	≈5	0·75	≈1
(residual pressure:	330	0·49	≈1
6×10^{-2} Pa)	475	0·55	≈1
	825	0·52	≈1
1300°C 24 h vacuum	≈5	1	3
(residual pressure:	800	very low	≈1
2×10^{-3} Pa)			
1100°C 29 h argon	≈5	0·76	≈1
(pressure: 70 kPa)	100	0·47	≈1
	>200	0·39	≈1

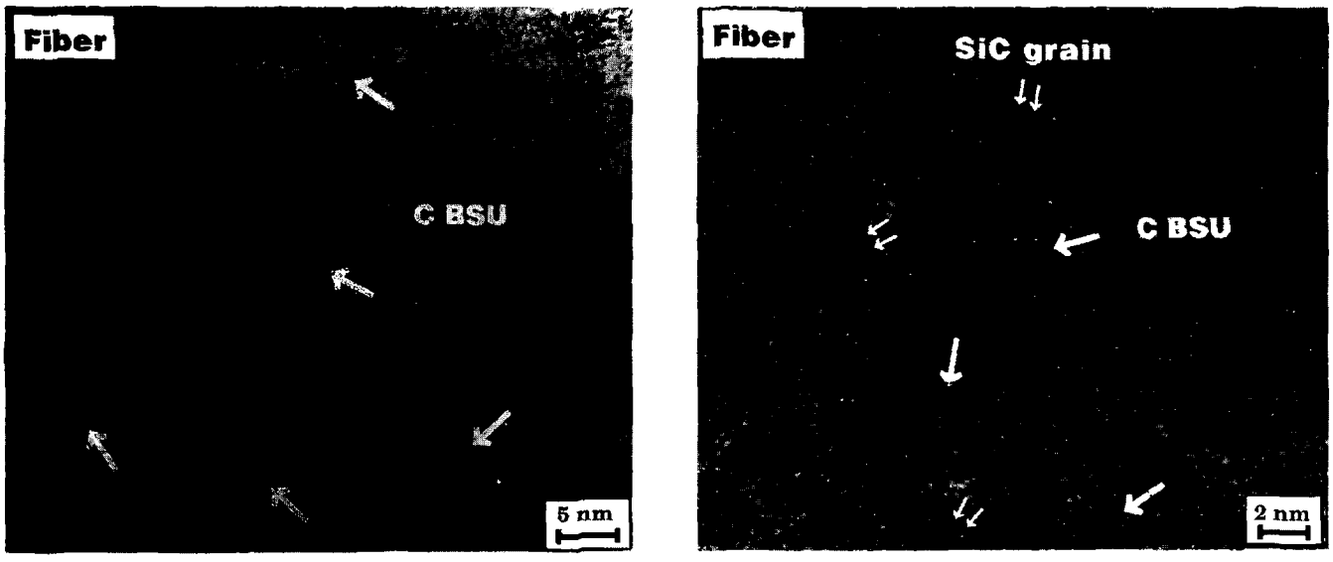

Fig. 12. TEM lattice fringe images of 2D SiC/C/SiC tensile test specimens which have been aged under vacuum at (a) 1100°C for 90 h (residual pressure: 6×10^{-2} Pa) and (b) 1200°C for 20 h (residual pressure: 10^{-1} Pa). The free carbon BSUs are shown with the single arrows and the SiC crystals with the double arrows.

that in the unaged composites, suggesting that the nature of the free carbon in the fibres has not changed during the ageing treatment [Fig. 12(a)].

Conversely, the nature of the FM interfacial zone is changed significantly when the composite is aged under more severe conditions (i.e. at 1200–1300°C with $\Delta m/m_0$ = 1–2%), as shown in Figs 13 and 14. First, some pyrocarbon from the initial interphase is still present (exclusively on the matrix side) but the majority of the carbon seems to have been consumed. Second, SiC crystals of large size (typically ≈ 20 nm) have been formed on the fibre surface. Furthermore, the AES depth concentration profiles (Fig. 14) show that the oxygen initially present in the fibres (as silicon oxycarbide) has been partly consumed over a depth of several 10 nm from the fibre surface, whereas both silicon and carbon atomic concentrations are now close to 50% (as in SiC). Finally, the TEM lattice fringe image [Fig. 12(b)] shows that within a zone of at least 1 μm from the fibre surface: (i) the carbon BSUs in the fibre are larger and more ordered and (ii) the SiC grain size is significantly enlarged (5 to 10 nm).

Finally, for still more severe ageing conditions (i.e. at 1200–1300°C and with $\Delta m/m_0$ >2%), the

Fig. 13. TEM image (bright-field) of the FM interfacial zone in a 2D SiC/C/SiC composite aged at 1200°C for 20 h under vacuum (residual pressure: 10^{-1} Pa).

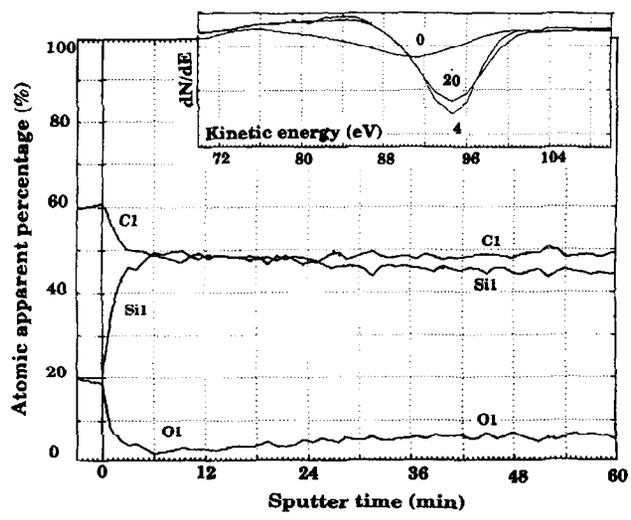

Fig. 14. AES depth concentration profiles recorded from the surface of a pulled-out fibre present at the failure surface of a tensile test specimen of a 2D SiC/C/SiC composite aged at 1300°C for 1 h under vacuum (residual pressure: 2×10^{-2} Pa). The etching rate was 8 nm min^{-1} (reference: Ta_2O_5). The shift of the Si_{LVV} transition as a function of etching time (0, 4 and 20 min) is shown in the inset.

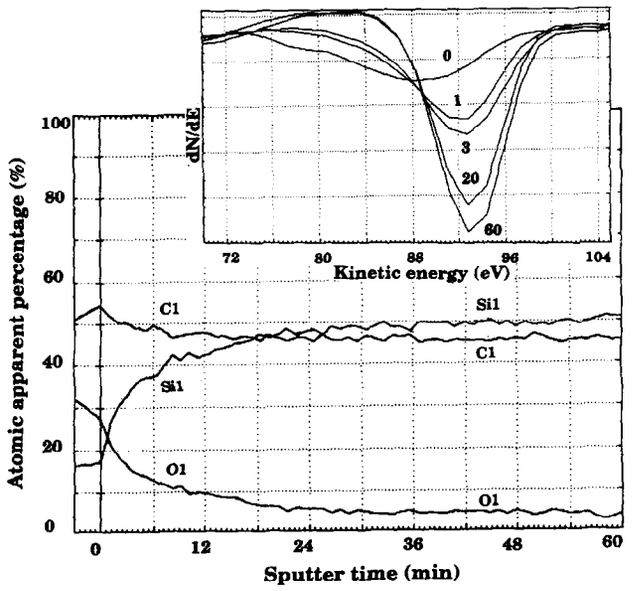

Fig. 15. AES depth concentration profiles recorded from the surface of a pulled-out fibre present at the failure surface of a tensile test specimen of a 2D SiC/C/SiC composite aged at 1200°C for 94 h under vacuum (residual pressure: 1×10^{-3} Pa). The etching rate was 8 nm min^{-1} (reference: Ta_2O_5). The shift of the Si_{LVV} transition as a function of etching time (0, 1, 3, 20 and 60 min) is shown in the inset.

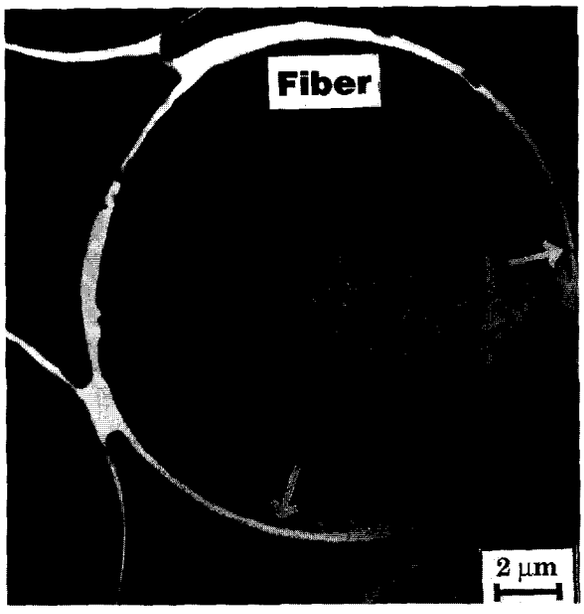

(a)

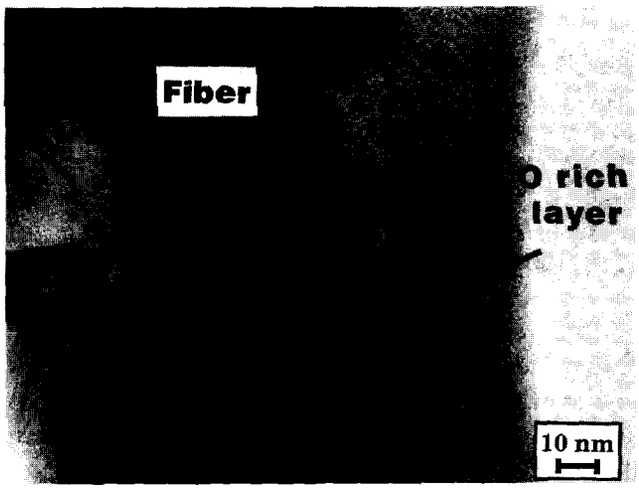

(b)

Fig. 16. TEM image [bright-field (a)] of a 2D SiC/C/SiC composite aged at 1200°C for 94 h under vacuum (residual pressure: 1×10^{-3} Pa), showing shrinkage of the fibres and (b) the occurrence of the SiO_2 + C layer formed on the fibre surface at locations indicated by the arrows.

pyrocarbon interphase has totally disappeared and the fibre is surrounded with a crown of large-sized SiC crystals. Additionally, for a high enough weight loss ($\Delta m/m_0$ = 6–7%), the fibre is significantly enriched in oxygen near its extreme surface (i.e. over a thickness of 30–40 nm) (Table 2, Figs 15 and 16), which might consist of a mixture of silica and carbon. Furthermore, significant shrinkage of the fibre occurs during ageing (Fig. 16) as the fibre undergoes decomposition (which consumes the oxygen of the oxycarbide phase) and tends towards a composition close to stoichiometric SiC (Table 2). For extremely severe ageing conditions (e.g. at 1460°C), the decomposition residue of the fibre undergoes pronounced grain growth [Fig. 9(c)] and exhibits an oxygen concentration which is almost nil.

3.3.3 Fibre bulk composition

The bulk composition of the fibre has been assessed by EPMA analysis. Its variations as a function of the ageing conditions are shown in Table 3 and Fig. 17. The data show that: (i) the evolution of the chemical composition seems to be uniform within the fibre (i.e. there is no radial composition gradient) and (ii) the evolution of the composition correlates with that of the weight loss, $\Delta m/m_0$. Finally, it is worth noting that the composition of the fibres tends towards that of pure silicon carbide for the most severe conditions, as already pointed out.

3.4 Mechanical behaviour after ageing

3.4.1 Under tensile loading

The stress–strain curves recorded at room temperature under tensile loading and representative of the mechanical behaviour of 2D SiC/C/SiC composites aged under various conditions, are shown in Fig. 18. For a given ageing temperature, e.g. 1100°C, the σ–ϵ curves exhibit the same general features for specimens aged under vacuum and treated under an argon atmosphere (Table 4).

After ageing under mild conditions (1100°C; $\Delta m/m_0$ = 0·4–1·3%), the composites exhibit a Young's modulus (defined as the slope of the σ–ϵ curve at the origin) which is almost the same as

Table 3. Bulk composition of SiC Nicalon fibres within 2D SiC/C/SiC composites aged under various conditions

Ageing treatment	$\Delta m/m_0$ (%)	*Composition (at%)*[c]			*C/Si at. ratio*
		Si	*C*	*O*	
None (as-received)	0	35	48	17	1·37
1100°C 29 h argon[a]	−0·37	35	48	17	1·40
1100°C 90 h vacuum[b]	−1·3	35	49	16	1·37
1200°C 20 h vacuum[b]	−2·05	44	49	7	1·11
1200°C 94 h vacuum[b]	−6·3	49	51	0	1·04
1300°C 24 h vacuum[b]	−6·9	47	52	1	1·11
1460°C 3 h vacuum[b]	−9·3	49	51	0	1·04

[a]Pressure: 70 kPa.
[b]Residual pressure: 10^{-1} to 10^{-3} Pa.
[c]Uncertainty: ≤ 1 at%.

that measured for the as-received materials (i.e. 200 ± 30 GPa). Conversely, both the stress corresponding to the end of the linear domain (σ_d) and the ultimate failure stress (σ_r) are significantly lower than those reported for the as-received composites (Section 3.1); i.e. σ_d = 60 MPa versus 90 MPa and σ_r = 120 MPa versus 150 MPa, respectively. Furthermore, the failure strain ϵ_r is much higher: 0·25 and 0·33% for the composites aged under argon (29 h) and vacuum (90 h) respectively, compared with only 0·17% for the as-supplied composites. Finally, the fibre pull-out is more pronounced for the aged composites. All these features suggest the occurrence of some weakening of the FM bonding.

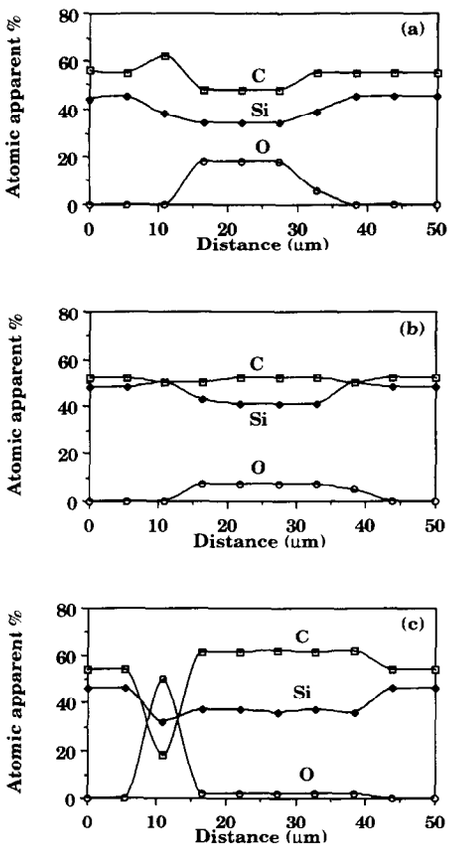

Fig. 17. EPMA radial concentration profiles in Nicalon fibres within 2D SiC/C/SiC composites which have been aged under vacuum (residual pressure: 10^{-1} to 10^{-3} Pa) and experienced various weight loss: (a) as-received composites or $\Delta m/m_0$ = −1·3% (1100°C, 90 h); (b) $\Delta m/m_0$ = −2% (1200°C, 20 h); and (c) $\Delta m/m_0$ = −7% (1300°C, 24 h).

The composites aged under more severe conditions, i.e. those corresponding to $\Delta m/m_0 \approx 2\%$ (e.g. for 1200°C/20 h), exhibit a mechanical behaviour that is significantly degraded with respect to that of the untreated specimens. Their σ–ϵ curves are still largely non-linear with a high failure strain (ϵ_r = 0·25 to 0·40%). However, their Young's modulus is reduced by about 30% and, more importantly, their failure stress is dramatically lowered (34 MPa instead of 146 MPa) (Table 4).

Finally, for still more severe conditions, corresponding to $\Delta m/m_0$(%) ranging from 3·6 to 7, all the aged composites exhibit brittle mechanical behaviour with an almost straight σ–ϵ curve and a very low failure strain (typically 0.015%).

3.4.2 Under push-out testing

Thin foils (thickness of about 250 μm) of the as-received composites and specimens aged under mild to moderate conditions ($\Delta m/m_0 \leq 2\%$) were submitted to push-out testing in order to assess the strength of the FM bonding (those corresponding to higher weight loss were too brittle).

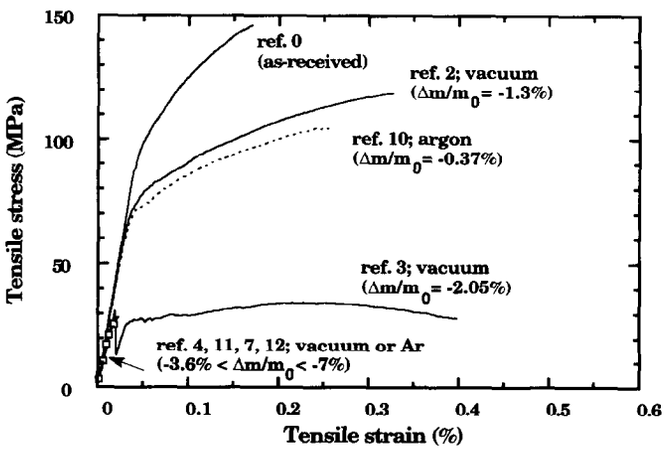

Fig. 18. Tensile stress–strain curves of 2D SiC/C/SiC composites tested at room temperature in the as-received state or after ageing treatments performed under various conditions.

Table 4. Mechanical characteristics measured at room temperature under tensile loading of 2D SiC/C/SiC composites in the as-received state and after ageing under various conditions

Ref.	*Ageing treatment*	$\Delta m/m_0$ *(%)*	σ_r *(MPa)*	ϵ_r *(%)*	E *(GPa)*
0	none (as received)	0	146	0·17	230
1	1100°C 50 h vac.	-0·55	—	—	—
2	1100°C 90 h vac.	-1·3	118	0·33	215
3	1200°C 20 h vac.	-2·05	34	0·25	160
4	1200°C 94 h vac.	-6·3	29	0·023	105
5	1300°C 1 h vac.	-1·5	45	0·36	170
6	1300°C 1·5 h vac.	-3·0	30	0·30	160
7	1300°C 24 h vac.	-6·9	26	0·012	—
8	1460°C 0·08 h vac.	-0·27	—	—	—
9	1460°C 3 h vac.	-9·3	—	—	—
10	1100°C 29 h Ar	-0·37	105	0·25	210
11	1200°C 49 h Ar	-3·58	25	0·015	170
12	1300°C 24 h Ar	-6·39	30	0·014	188

The load–displacement curves are shown in Fig. 19 in their as-recorded state, for four materials corresponding to increasing values of $\Delta m/m_0$ (Table 5). Each curve, e.g. that for the as-received material, can be analysed as follows. The first non-linear part of the curve (for $F < F_d$) corresponds to the penetration of the Vickers indentor into the Nicalon fibre. Beyond F_d, progressive decohesion of the FM interface takes place with a significant change in the slope of the curve. The value of F_d (defined as the load corresponding to the beginning of FM interface debonding) depends on the interface toughness and the residual clamping stress.[23] Total debonding of the FM interface is achieved when the applied load is equal to a critical value, referred to as F_c. This value depends strongly on the thickness of the thin foil.[23–27] Beyond F_c, the fibre, which is now debonded over its full length (i.e. the thickness of the foil), undergoes pure sliding with respect to the matrix. Since use of the classical models proposed to derive interface parameters (Marshall and Oliver model) from push-out test data[23–27] could be questioned in the present case (owing to the occurrence of relatively strong FM bonding and thick interphase), F_d and F_c were retained to follow, on a comparative basis, the evolution of the FM bonding during the ageing treatment.

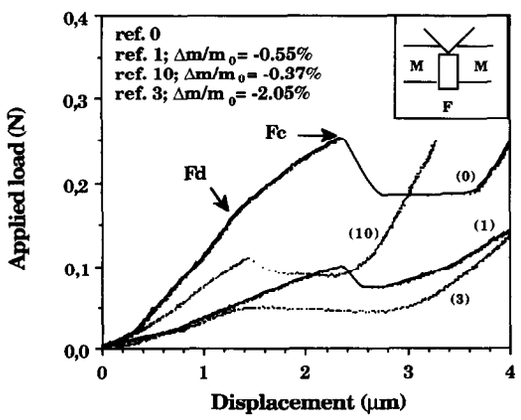

Fig. 19. Representative load–displacement push-out test curves recorded for 2D SiC/C/SiC composites (250 μm thin foils) in the as-received state (ref. 0) or aged under conditions of increasing $\Delta m/m_0$ (ref. 1, 10, 3). F_d—load at beginning of FM decohesion; F_c—load at fibre sliding. The loading device is shown in inset.

In the composites submitted to mild ageing conditions, i.e. corresponding to $\Delta m/m_0$ = 0·4–0·5%, there is already a significant decrease in the values of both F_d and F_c (i.e. about 30 and 50% respectively). This decrease becomes much more dramatic for the composites aged under moderate conditions ($\Delta m/m_0 \approx 2\%$). For these latter materials, the depth of the Vickers indentation in the fibres is very small, the values of F_d and F_c are almost the same and the fibres start sliding almost as soon as load is applied to the indentor. All these features show that the FM bonding is obviously significantly reduced for ageing characterized by weight loss as low as 2%.

Finally, it is worthy of note that the decrease in the values of F_d and F_c correlates with that observed in the value of σ_d, the tensile stress corresponding to the end of the linear elastic domain (Table 5).

4 Discussion

For the purpose of comparison, ageing treatments were performed under vacuum at 1400°C, on the SiC CVI matrix alone. The SiC sample was deposited under the CVI conditions used in the present work for infiltration of the SiC matrix into the fibre preforms. However, the deposition was carried out as a CVD coating on the external surface of a flat substrate and then the SiC coating was detached mechanically from the substrate. Such a SiC sample exhibited no weight loss during the ageing treatment (as expected).

Table 5. Push-out test data (F_d, F_c) for 2D SiC/C/SiC in the as-received state or after ageing under mild or moderate conditions. The weight loss $\Delta m/m_0$ and the tensile failure stress are also given. Each value of F_d and F_c is the mean of 15–20 individual data recorded for 15 μm fibres

Ref.	*Ageing treatments*	$\Delta m/m_0$ *(%)*	F_d *(N)*	F_c *(N)*	σ_d^a *(MPa)*
0	none (as-received)	0	0·17 ± 0·02	0·29 ± 0·04	85
1	1100°C 50 h vac.	−0·55	0·13 ± 0·02	0·16 ± 0·04	55
10	1100°C 29 h Ar	−0·37	0·11 ± 0·02	0·13 ± 0·04	55
3	1200°C 20 h vac.	−2·05	0·04 ± 0·02	0·05 ± 0·02	30

[a]As derived from tensile test.

Furthermore, the maximum weight loss recorded under extremely severe ageing conditions (i.e. at 1550°C) for 2D SiC/C/SiC composites corresponds to a value of $\Delta m/m_f$ (where m_f is the fibre mass in the composite sample) of about 27%, as already mentioned in Section 3.2. It is noteworthy that this value is close to those previously reported for the bare Nicalon fibres (ceramic grade) themselves[22] or obtained in the present work for the as-received Nicalon fabrics (Fig. 6).

Thus one may conclude that the weight losses observed during the ageing treatments performed on the 2D SiC/C/SiC composites (Fig. 5) and the related variations in their mechanical behaviour (Fig. 18) are mainly due to the evolution of the fibres and the FM interfacial zone (including the PyC interphase), as will be discussed in the present section.

4.1 Degradation of the fibre in the bulk

The TEM images [Figs 9(a)–(c)] clearly show that the Nicalon fibres undergo a crystallization process when 2D SiC/C/SiC composites are aged beyond 1100°C under vacuum or argon, the main result of which is uniform growth of SiC crystals in the bulk of the fibres. The mean size of the SiC crystals correlates with both the weight loss experienced by the composite (Fig. 8) and the residual oxygen concentration in the fibres as assessed by EPMA (Table 3). It increases regularly as $\Delta m/m_0$ becomes more and more significant, correlating with a decrease in the oxygen concentration in the fibres. Additionally, there is at least for the fibres that were moderately degraded (i.e. for $\Delta m/m_0 \approx$ 2%), some reorganization of the BSUs in the free carbon phase [Figs 12(a) and (b)].

The thermal degradation of the fibres as observed during the ageing of 2D SiC/C/SiC composites under vacuum or argon exhibits features that are close to those previously reported for the bare Nicalon fibres themselves.[8–10] It is well established that the ternary Si–C–O fibres undergo an overall compositional and microstructural evolution beyond about 1100°C, with the formation of large SiC crystals and a decrease in their oxygen concentration. The primary phenomenon is the decomposition of silicon oxycarbide (written as SiO_xC_y or better $SiO_{2x}C_{1-x}$)[18] with an evolution of gaseous species (mainly CO and SiO),[6–8,12] which can in turn react with the solid species and particularly the free carbon. As both the silicon oxycarbide (which acts as a matrix in the as-processed fibres, thus keeping the SiC nanocrystals isolated from one another) and the free carbon are progressively consumed, grain growth can occur in the silicon carbide phase. This grain growth is a function of the temperature and duration of the ageing treatment.[8,13]

During the ageing treatments, various secondary reactions involving the gaseous CO and SiO species resulting from the primary decomposition of silicon oxycarbide may occur depending upon the local conditions. Those corresponding to the following equations are characterized by negative $\Delta G°$ values within the 1100–1400°C temperature range, and are thus possible from a thermodynamic standpoint.[28]

$$SiO(g) + 2\,C(s) \rightarrow SiC(s) + CO(g) \quad (1)$$

$$2\,SiO(g) + C(s) \rightarrow SiO_2(s) + SiC(s) \quad (2)$$

$$2\,CO(g) + SiC(s) \rightarrow SiO_2(s) + 3\,C(s) \quad (3)$$

$$SiO(g) + CO(g) \rightarrow SiO_2(s) + C(s) \quad (4)$$

$$3\,SiO(g) + CO(g) \rightarrow 2\,SiO_2(s) + SiC(s) \quad (5)$$

Analyses performed on Nicalon fibres in 2D SiC/C/SiC composites aged under vacuum beyond 1200°C, by TEM and EPMA, show that the fibres undergo a compositional/microstructural evolution with the following features: (i) it is homogeneous in the bulk of the fibre (i.e. there are no gradients), (ii) there is a simultaneous decrease in both the oxygen and carbon concentrations and (iii) SiC grain growth occurs. Furthermore, the AES analyses (inset in Fig. 15) show that the Si_{LVV} transition falls at about 93 eV when recorded after a sufficiently long etching time (e.g. 60 min), i.e. sufficiently deep within the fibre (≈500 nm from the fibre surface; Ta_2O_5 standard). This value better corresponds to that reported for SiC (92 eV)

than for SiO_2 (75 eV), as previously mentioned by Vine and Steeds.[29] On the basis of these data, the secondary reactions yielding silica [i.e. eqns (2) to (5)] seem to be unlikely.

Thus, it seems more appropriate to assume that the decrease in both the oxygen and carbon concentrations in the bulk of the fibres (Table 3) might be related to the formation of CO according to the following primary and secondary equations:

$$SiO_{2x}C_{1-x} \rightarrow SiO(g) + (2x - 1)\,CO(g) + (2 - 3x)\,C(s) \quad (6)$$

$$SiO(g) + 2C(s) \rightarrow SiC(s) + CO(g) \quad (1)$$

where the carbon present in the left-hand side of eqn (1) includes the free carbon of the fibres.

The assumption that CO is the main gaseous species formed during decomposition of the fibres and responsible for the decrease in both the oxygen and carbon concentrations in the fibres, is further supported by comparing the compositions of the fibres in the aged and as-received composites (Table 3). For a given ageing treatment (e.g. 20 h at 1200°C under vacuum), one can calculate (as shown in Table 6) from the composition of the as-received fibres (line 1) the corresponding numbers of moles of CO and SiO [and, by difference, those of Si, C and O in the solid (line 2)] necessary to achieve the best fit between the resulting theoretical composition of the aged fibres (line 3) and that established experimentally by EPMA (line 4 and Table 3). Thus, for a first example corresponding to a rather low $\Delta m/m_0$ value ($\approx 2\%$; Table 3), the result of the calculations is 10 moles of CO for 1 mole of SiO. Thus the majority of the SiO species formed according to eqn (6) reacts *in situ* with carbon, and CO is indeed the main gaseous product of the fibre decomposition.

Similar calculations (Table 6) show that a more significant evolution of SiO might occur for more severe ageing treatment, e.g. 94 h at 1200°C under vacuum with $\Delta m/m_0 \approx 6\%$ (Table 3). For such conditions, the best fit is achieved by assuming an evolution of 14 moles of CO and 3 moles of SiO. The evolution of SiO might be more favoured here since the free carbon is almost totally consumed (C/Si (at) $\approx$ 1·04 versus 1·31 for the as-received fibres) and the resulting fibre porosity large enough.

The decrease in volume of the fibre solid phases, resulting from the decomposition of silicon oxycarbide and the reaction of SiO with free carbon, might thus explain: (i) the slight local decohesions observed at the fibre–pyrocarbon interface in composites aged under mild conditions [with $\Delta m/m_0 < 1\%$; Figs 10(a) and (b)] and (ii) the important fibre shrinkage clearly apparent from the TEM image (Fig. 16) for the composite aged under severe conditions (with $\Delta m/m_0 \approx 6\%$). For this latter case, the consumption of the PyC interphase (to be discussed in the next section) cannot explain alone the large void between the fibre and matrix, which is thus mainly due to shrinkage of the fibre.

4.2 Reactions at the FM interface

The experimental data reported in Section 3.3 show that, during composite ageing, the surface of the Nicalon fibre undergoes an evolution which is somewhat different from that of the bulk. As a matter of fact, the fibre surface appears to be a

Table 6. Evolution of the chemical composition of the fibre (in the bulk) in uncoated 2D SiC/C/SiC composites aged under vacuum. The nature and mole numbers of species removed from the initial composition have been determined semi-empirically to achieve the best fit with the experimental composition in the aged composites (as assessed by EPMA)

	Species removed	*Composition in fibre bulk (at%)*		
		Si	*C*	*O*
(a) 1200°C 20 h vacuum (10^{-1} Pa)				
in as-received material		35	48	17
assumed ageing model	10 CO (g) 1 SiO (g)	34	38	6
calculated composition		43·6	48·7	7·7
experimental composition		44	49	7
(b) 1200°C 94 h vacuum (10^{-3} Pa)				
in as-received material		35	48	17
assumed ageing model	14 CO (g) 3 SiO (g)	32	34	0
calculated composition		48·5	51·5	0
experimental composition		49	51	0
(c) 1300°C 24 h vacuum (2×10^{-3} Pa)				
in as-received material		35	48	17
assumed ageing model	13 CO (g) 3 SiO (g)	32	35	1
calculated composition		47	51·5	1·5
experimental composition		47	52	1

particular reaction site where the Si–C–O system (i.e. the fibre is in contact with either a pure carbon medium or a gaseous phase of unknown composition, depending on whether the pyrocarbon interphase is still present or has been totally consumed.

As long as $\Delta m/m_0 < 1\%$ (i.e. for mild ageing conditions), the PyC interphase is still present at the FM interface. TEM (Fig. 10) and AES (Fig. 11) data show that the 5–10 nm thick C/SiO_2 layer is still present at the fibre surface, and the nanotexture of the PyC interphase is basically unchanged. Thus, the interactions between the gaseous products of fibre decomposition (formed in very low amounts under such conditions) and the FM interfacial zones remain too limited to alter the constituents significantly.

Conversely, when $1 < \Delta m/m_0 < 2\%$ (i.e. for T = 1200°C), growth of SiC crystals takes place which is much more significant at the fibre surface than in the bulk of the fibres (Figs 12 and 13). Simultaneously, the oxygen concentration decrease in the fibre is more pronounced near the fibre surface than in the bulk (Fig. 14), on the one hand, and the carbon atomic layers from the PyC interphase are consumed on the fibre side (Fig. 13), on the other hand. Last, both the TEM image (Fig. 13) and AES analysis (Fig. 14) show that silica is no longer present at the fibre surface. All these features can be explained by assuming that the fibre decomposition gaseous products (and particularly SiO) react with the carbon from the interphase to give a crown of large SiC crystals (Fig. 13) with an evolution of mainly carbon monoxide. Thus, the reaction scheme given previously for the bulk of the fibre, namely a combination of eqns (6) and (1), still seems to be valid (the carbon from the left-hand side of eqn (1) including now part of the interphase pyrocarbon).

Finally, when $\Delta m/m_0 > 2\%$ (i.e. for severe ageing conditions), the pyrocarbon interphase is totally consumed according to eqn (1) and consequently a rather thick layer (50–80 nm) of large SiC crystals is present at the fibre surface [Figs 16(a) and (b)]. These results are consistent with those reported for the ageing of 2D SiC/C/SiC composites under argon (P = 100 kPa) by Mozdzierz and Backhaus-Ricoult[30] or vacuum (residual pressure 10^{-3} Pa) by Vine and Steeds.[29] Moreover, the fact that there is an oxygen accumulation at the fibre surface and the formation of an amorphous layer outside the SiC crystal layer [Figs 15 and 16(b)], for long ageing times, suggests that the fibre surface is still the site of chemical reactions (still involving the fibre decomposition products, i.e. SiO or/and CO[31] even when the PyC interphase is totally consumed. However, under such new conditions, the Si–C–O system (i.e. the fibre) is in contact with a gaseous phase and the secondary reactions are different. TEM/PEELS and AES analyses (Table 2 and Fig. 15) have shown that the amorphous layer formed outside the SiC crystal layer [Fig. 16(b)] can be assigned to a mixture of silica and carbon. The fact that the reaction leading to the formation of this layer takes place only on the fibre surface and not within the bulk of the fibre (although it is highly porous and largely made of SiC), suggests that the new secondary reaction might be that according to eqn (4).

4.3 Weight loss kinetics

As shown in Fig. 5, 2D SiC/C/SiC composites experience a weight loss $\Delta m/m_0$ when they are aged at a sufficiently high temperature under vacuum or argon. This weight loss can be assigned to decomposition of the fibres and to reactions occurring between the gaseous decomposition products of the $SiO_{2x}C_{1-x}$ species and free carbon (from the fibres and the interphase), as discussed in Sections 4.1 and 4.2. Furthermore, the contribution of fibre decomposition to the weight loss is expected to be much larger than that of the reaction of the pyrocarbon interphase with SiO [eqn (1)], owing to the values of the related volume fractions in the composites (i.e. $V_f \approx 40\%$). These assumptions are clearly supported by several experimental results. First, the weight loss starts at the same temperature, i.e. ≈ 1100°C, for both the composites (Fig. 5) and the related bare fabrics (Fig. 6), in agreement with data reported previously for Nicalon fibre.[11–13] Second, the maximum absolute weight loss Δm recorded for extremely severe ageing treatments (T = 1550°C; vacuum), when expressed with respect to the fibre mass present in the composite (with $V_f \approx 40\%$), i.e. as $\Delta m/m_f$, corresponds to a value (≈27%) close to that reported for complete decomposition of bare Nicalon fibres.[22] This latter result obviously shows that the majority of the weight loss is related to the decomposition of the fibres.

The weight loss rate and the kinetic regime depend on the conditions of the ageing treatments, as shown in Figs 5–7. For not too severe ageing conditions (i.e. $T < 1300$°C; $\Delta m/m_0 < 8\%$), the variations of $\Delta m/m_0$ as a function of the square root of time are linear [Fig. 5(b)], as they are for the related bare Nicalon fabrics (inset in Fig. 6). This feature suggests that, under such conditions, the rate-limiting step might be a diffusion process the nature of which still remains unknown. Conversely, for extremely severe ageing conditions (T = 1460°C; vacuum; $8 < \Delta m/m_0 < 11\%$), the linear $\Delta m/m_0 = f(\sqrt{t})$ relation is no longer valid and the diffusion rate-controlling step no longer

effective. Tentatively, this change in the kinetic regime might be related to the fact that the fibres and FM interfacial zones exhibit a very high porosity for such $\Delta m/m_0$ values.

The effect of the ageing treatment atmosphere on the weight loss rate and kinetics is shown in Fig. 7. For treatments performed under vacuum, the apparent activation energy E_a is about the same (i.e. 190 kJ mol^{-1}) for both the composites and the related bare Nicalon fabrics, suggesting that the rate-limiting step is the same. Conversely, for a given ageing temperature, e.g. 1200°C, the kinetic (or diffusion-based) constant is much higher for the bare fibres. Thus the weight loss and the decomposition/reaction process are slowed down in a significant manner when the fibres are embedded within the SiC matrix, as would be expected for a process involving an evolution of gaseous species (namely CO and SiO).

The weight loss kinetics corresponding to ageing treatments performed under vacuum or argon exhibit both common features and differences, as is apparent from Figs 5 and 7. The common features, i.e. the shape of the $\Delta m/m_0 = f(t)$ curves, might be related to the fact that both media are non-reacting atmospheres with respect to the composites. The differences, namely the lower weight loss rates (Fig. 5) and the high apparent activation energy (Fig. 7) observed for the ageing treatments performed under argon, might be related to the effect of pressure on the decomposition/reaction process. Tentatively, under a pressure of 70 kPa of argon, the equilibria involving the CO and SiO gaseous species either within the fibres or the FM interfacial zones might be affected, with the result that the decomposition/reaction process responsible for the weight loss is slowed down. However, this pressure effect—which is pronounced at low temperatures—tends to decrease as the temperature is raised (at 1300°C, the weight loss kinetics are similar) (Fig. 5).

4.4 Effect of ageing on the mechanical behaviour

The chemical and microstructural evolution that occurs versus time during the ageing treatments of 2D SiC/C/SiC composites, in the fibres and FM interfacial zones, results in a degradation of the mechanical behaviour of the composites at room temperature, as shown in Figs 18 and 19. This degradation remains moderate for mild ageing conditions ($0{\cdot}37 < \Delta m/m_0 < 1{\cdot}3\%$) and becomes dramatic when they are more severe ($2 < \Delta m/m_0 < 7\%$). It can be assigned to a lowering of the FM bonding and a decrease of the fibre strength due to a decomposition/grain growth process.

For mild ageing conditions (1100°C; $0{\cdot}37 < \Delta m/m_0 < 1{\cdot}3\%$), the decrease in the value of σ_d (Fig. 18 and Table 5) can be explained by a lowering of the FM bonding (Fig. 19 and Table 5) as suggested by the occurrence of decohesion between the fibre and the anisotropic layer of the pyrocarbon interphase [Figs 10(a) and (b)]. Although the effect of ageing seems to remain limited in terms of chemical and microstructural change, the strength of the FM bonding and the load-transfer capability of the interface are already lowered in a significant manner, as supported by the push-out data (F_d and F_c being reduced by about 30 and 50%, respectively, for $\Delta m/m_0 \approx 0.5\%$). Conversely, under such ageing conditions (i.e. for $0{\cdot}37 < \Delta m/m_0 < 1{\cdot}3\%$), the SiC grain growth in the fibre remains very limited (Fig. 8), with the result that the failure stress of the fibres and thus that of the composite is not degraded in a dramatic manner (Fig. 18). Finally, by lowering the FM bonding the ageing treatment has a positive effect on the failure strain of the composite, which is observed to increase by $\approx 47\%$ for $\Delta m/m_0 = 0{\cdot}37\%$ and by almost 100% for $\Delta m/m_0 = 1{\cdot}3\%$ (Fig. 18 and Table 4).

For more severe ageing conditions (corresponding to $\Delta m/m_0 \approx 2\%$, e.g. for 20 h at 1200°C under vacuum), the effect of the treatment on the mechanical behaviour becomes dramatic, particularly in terms of load-bearing capability (σ_r being reduced from 146 to 34 MPa) (Table 4). This reduction of the failure strength of the composite is related to the fact that: (i) the fibres are almost totally debonded from the matrix (Fig. 19), the pyrocarbon interphase being largely consumed by reaction with SiO (Fig. 13) and (ii) large crystals of SiC are already present at the fibre surface which may act as surface flaws, thus lowering the fibre failure strength. However, these somewhat weakened fibres can still carry moderate load level at a high strain ($\approx 0{\cdot}3\%$) since they are no longer bonded to the matrix.

Finally, for extremely severe ageing conditions (corresponding to $3{\cdot}6 < \Delta m/m_0 < 7\%$), the composites exhibit a brittle behaviour which can be explained by the absence of any FM bonding and the extreme degradation state of the fibres (which are now porous and made of large SiC-crystals). The absence of FM bonding is related to both the shrinkage of the fibres (Fig. 16) and the consumption of the pyrocarbon interphase, related to chemical reaction [eqn (1)] between SiO and carbon.

There is thus a good correlation between the weight loss experienced by the composites during the ageing treatments (associated with decomposition of the Nicalon fibres and side reactions) on the one hand, and the change in the mechanical behaviour of the composites (itself related to

weakening of both the fibre strength and FM bonding) on the other hand.

5 Conclusions

From the data which have been presented in Section 3 and discussed in Section 4, the following conclusions can be drawn.

(i) 2D SiC/C/SiC composites aged at a sufficiently high temperature under vacuum or argon undergo a weight loss which increases as temperature and time are raised. This weight loss is related to decomposition of the silicon oxycarbide present in Nicalon fibres and to side-reactions between the gaseous decomposition products (i.e. SiO) and the free carbon from the fibres themselves and the pyrocarbon interphase. As this decomposition proceeds, the oxygen and carbon concentrations in the fibres decrease and simultaneously grain growth of the SiC crystals occurs.

(ii) The ageing treatments also result in a change in the mechanical behaviour of the composites which is related to a weakening of the fibre–matrix bonding and fibre strength, itself a consequence of the decomposition/reaction process occurring in the fibres and the fibre–matrix interfacial zone.

(iii) For mild ageing conditions, corresponding to $\Delta m/m_0 < 1{\cdot}3\%$, there is a decrease in the proportional limit σ_d and an increase in the failure strain ϵ_r; these are related to a weakening of the fibre–matrix bonding which may itself be related to the occurrence of decohesion at the fibre–pyrocarbon interface. Under such ageing conditions, the load-bearing capability of the composites remains relatively high since the decomposition/recrystallization process of the fibres is still limited.

(iv) For more severe ageing conditions, corresponding to a weight loss of about 2%, the failure strength of the composites is dramatically lowered. This feature is related to the fact that the fibres are largely debonded from the matrix (the pyrocarbon interphase being partly consumed by reaction with SiO) and exhibit large SiC crystals on their surface, formed by reaction between SiO and the pyrocarbon, and acting as surface flaws. Conversely, the failure strain of the composites is significantly improved.

(v) For extremely severe ageing conditions, corresponding to $3 < \Delta m/m_0 < 7\%$, all the composites exhibit brittle behaviour due to the absence of any bonding between the fibres and matrix, and more importantly to an extreme weakening of the fibres.

Acknowledgements

This work was performed within the framework of the national cooperative research programme entitled 'Thermomechanical Behavior of Ceramic Matrix Composites' (GS-4C), supported by CNES, DRET, MRES, Aerospatiale, SEP and SNECMA. The authors are indebted to L. Guillaumat and B. Humez (LCTS) for their contribution to the mechanical tests, M. Lahaye and M. Chambon (CUMEMSE, Univ. Bordeaux) for their assistance in the AES and TEM analyses, and Y. Kihn (CEMES-LOE, CNRS, Toulouse) for her contribution to the EELS analysis. They acknowledge the assistance received from SEP through the supply of samples and valuable discussions with P. Olry, S. Loison and J. M. Jouin.

References

1. Yajima, S., Okamura, K., Hayashi, J. & Omori, M., Synthesis of continuous SiC fibers with high tensile strength. *J. Am. Ceram. Soc.*, **59**[7–8] (1976) 324–327.
2. Guigon, M., Microtexture de fibres de carbure de silicium. Etude par microscopie électronique par transmission. *Rev. de Phys. Appl.*, **23** (1988) 229–238.
3. Guigon, M., Structure et microtexture de fibres de carbure de silicium. *La Recherche Aérospatiale*, **3** (1989) 9–19.
4. Laffon, C., Flank, A. M., Lagarde, P., Laridjani, M., Hagege, R., Olry, P., Cotteret, J., Dixmier, J., Miquel, J. L., Hommel, H. & Legrand, A. P., Study of Nicalon-based ceramic fibres and powders by EXAFS spectrometry, X-ray diffractometry and some additional methods. *J. Mater. Sci.*, **24**[4] (1989) 1513–1522.
5. Sawyer, L. C. & Arons, R., Characterization of Nicalon: strength, structure and fractography. *Ceram. Eng. Sci. Proc.*, **7–8** (1985) 567–575.
6. Rocabois, P., Multiple Knudsen cell mass spectrometric investigation of the evaporation of silicon oxycarbide glass. International Conference on Metallurgical Coating and Thin Films (ICMCTF 93), San Diego, 19–24 April 1993; *Surf. Coatings Technol.*, in press.
7. Rocabois, P., Chatillon, C. & Bernard, C., Mass spectrometry experimental investigation and thermodynamic calculation of the Si–C–O system and Si_x–C_y–O_z fibre stability. *HT-CMC 93*, eds R. Naslain, J. Lamon and D. Doumeingts. Woodhead Publishers, Cambridge, 1993, pp. 93–100.
8. Mah, T. & Hecht, N. L., Thermal stability of SiC fibres (Nicalon). *J. Mater. Sci.*, **19** (1984) 1191–1201.
9. Clark, T. J. & Arons, R. M., Thermal degradation of Nicalon SiC fiber. *Ceram. Eng. Sci. Proc.*, **6**[7–8] (1985) 576–588.
10. Sawyer, L. C. & Chen, R. T., Thermal stability characterization of SiC ceramic fibers: II, fractography and structure. *Ceram. Eng. Sci. Proc.*, **7**[7–8] (1986) 914–930.
11. Ishikawa, T. & Ichikawa, H., Strength and structure of SiC fiber after exposure to high temperature. *Proc. Electrochem. Soc.*, **85**[5] (1988) 205–217.
12. Johnson, S.M., Degradation mechanisms of silicon carbide fibers. *J. Am. Ceram. Soc.*, **71**[3] (1988) C132–C135.

13. Jaskowiak, M. H. & DiCarlo, J. A., Pressure effects on the thermal stability of silicon carbide fibers. *J. Am. Ceram. Soc.*, **72**[2] (1989) 192–197.
14. Bouillon, E., Langlais, F., Pailler, R., Naslain, R., Sarihou, J. C., Delpuech, A., Laffon, C., Lagarde, P., Cruege, F., Huong, P. V., Monthioux, M. & Oberlin, A., On the conversion mechanisms of a polycarbosilane precursor into a SiC-based ceramic material. *J. Mater. Sci.*, **26** (1991) 1333–1345.
15. Bouillon, E., Mocaer, D., Villeneuve, J. F., Pailler, R., Naslain, R., Monthioux, M., Oberlin, A., Guimon, C. & Pfister, G., Composition–microstructure–property relationships in ceramic monofilments resulting from the pyrolysis of a polycarbosilane precursor at 800–1400°C. *J. Mater. Sci.*, **26** (1991) 1517–1530.
16. Bibbo, G. S., Benson, P. M. & Pantano, C. G., Effect of carbon monoxide partial pressure on the high temperature decomposition of Nicalon fibre. *J. Mater. Sci.*, **26**[18] (1991) 5075–5080.
17. Bodet, R., Microstructural instability and the resultant strength of Si–C–O and Si–N–C–O based ceramic fibers. Thèse de Master en Sciences des Matériaux Céramiques, Department of Materials Science, The Pennsylvania State University, 1991.
18. Bodet, R., Comportement en fluage et évolution microstructurale de fibres issues de précurseurs organosiliciés. Thèse n° 986, Univ. Bordeaux I, 1993.
19. Naslain, R. & Langlais, F., CVD-processing of ceramic–ceramic composite materials. In *Tailoring Multiphase and Composite Ceramics*, eds R. E. Tressler, G. L. Messing, C. G. Pantano & R. E. Newnham. Plenum Press, New York, *Mater. Sci. Res.*, **20** (1986) 145–164.
20. Cojean, D., Monthioux, M. & Oberlin, A., Phénomènes interfaciaux dans des composites SiC/SiC 2D de propriétés mécaniques variées. *Actes JNC7*, eds G. Fantozzi & P. Fleischmann. AMAC, Paris, 1990, pp. 381–390.
21. Naslain, R., Fiber–matrix interphases and interfaces in ceramic matrix composites processed by CVI. *J. Compos. Interfaces*, **1**[3] (1993) 253–286.
22. Le Coustumer, P., Monthioux, M. & Oberlin, A., Understanding Nicalon fibre. *J. Eur. Ceram. Soc.*, **11** (1993) 95–103.
23. Kerans, R. J., Theoretical analysis of the fiber pullout and pushout tests. *J. Am. Ceram. Soc.*, **74**[7] (1991) 1585–1596.
24. Cranmer, D. C., Deshmukh, U. V., & Coyle, T. W., Comparison of methods for determining fiber/matrix interface frictional stresses in ceramic matrix composites. In *Thermal and Mechanical Behavior of Metal Matrix and Ceramic Matrix Composites*, ASTM STP 1080, eds J. M. Kennedy, H. H. Moeller & W. S. Johnson. American Society for Testing and Materials, Philadelphia, 1990, pp. 124–135.
25. Shetty, D. K., Shear-lag analysis of fiber push-out (indentation) tests for estimating interfacial friction stress in ceramic-matrix composites. *J. Am. Ceram. Soc.*, **71**[2] (1988) C107–109.
26. Weihs, T. P. & Nix, W. D., Experimental examination of the push-down technique for measuring the sliding resistance of silicon carbide fibers in a ceramic matrix. *J. Am. Ceram. Soc.*, **74**[3] (1991) 524–534.
27. Weihs, T. P., Sbaizero, O., Luh, E. Y. & Nix, W. D., Correlating the mechanical properties of a continuous fiber-reinforced ceramic-matrix composite to the sliding resistance of the fibers. *J. Am. Ceram. Soc.*, **74**[3] (1991) 535–540.
28. JANAF *Thermochemical Tables*, third edition, eds M. W. Chase, C. A. Davies, J. R. Downey, D. J. Frurip, R. A. McDonald & A. N. Syverud. American Chemical Society and American Institute of Physics, 1985, Vol. 14.
29. Vine, W. J. & Steeds, J. W., The microstructure of silicon carbide (Nicalon) fibre reinforced silicon carbide ceramic-matrix composites heat-treated in vacuo and in pure oxygen. *J. Microsc.*, **169** (1993) 207–213.
30. Mozdzierz, N. & Backhaus-Ricoult, M., Effect of oxygen activity on the microstructure of 2D-SiC/C/SiC composites at high temperature. *Actes JNC8*, eds O. Allix, J. P. Favre & P. Ladevèze. AMAC, Paris, 1992, pp. 225–239.
31. Delverdier, O., Monthioux, M. & Oberlin, A., The role of oxygen in the thermal behaviour of polycarbosilane-based ceramics. *Actes JNC 7*, eds G. Fantozzi & P. Fleischmann. Paris, 1990, pp. 391–400.